


Analysis of relationship between soil erosion and lake deposition during the Holocene in Xingyun Lake, southwestern China

The Holocene
2021, Vol. 31(9) 1391–1400
© The Author(s) 2021
Article reuse guidelines:
sagepub.com/journals-permissions
DOI: 10.1177/09596836211019089
journals.sagepub.com/home/hol


Hongfei Zhao,¹  Jie Zhou,² Qianli Sun,³ Claudio O Delang,⁴
Ali Mokhtar,¹ Yue Ma¹ and Hongming He^{1,5}

Abstract

Quantifying the relative influences of anthropogenic activities and climate change on soil erosion and deposition during the Holocene, when both forces have been interacting is a complex problem. Analysis of long-term patterns in soil erosion and lake deposition in a basin can provide the basis for untangling the complexities of climate and anthropogenic forcings. In this paper, sedimentary sequences from Xingyun Lake are compared with simulated soil erosion rates in the basin to explore the relationship between river basin soil erosion and lake deposition during the Holocene in Yunnan, China. Modern soil erosion rates are calculated using RUSLE, while Holocene soil erosion rates are estimated using modern rates with reconstructed precipitation and vegetation cover sequences. Through this investigation, we found the following results. First, Holocene vegetation in the lake basin was mainly affected by climate change, and the vegetation experienced the same pattern of changes as the climate. Soil erosion and lake deposition rates, along with changes to vegetation cover, were synchronous with precipitation trends during the Holocene. Second, soil erosion and lake deposition have been exacerbated by human activities, such as deforestation and land reclamation in the Xingyun Lake basin. Finally, this study provides new insights into the effects by anthropogenic impacts and climate forcing on the processes of soil erosion and lake deposition on the millennium scale.

Keywords

climate change, Holocene, lake deposition, lake sediment, soil erosion, Yunnan

Received 14 November 2020; revised manuscript accepted 7 April 2021

Introduction

Soil erosion is a process affected by precipitation, vegetation, soil characteristics, topography, and human activities and is widely recognized as a response to climate variability and human activities (Dotterweich, 2013; Nearing et al., 2017). Environmental factors, such as climate and vegetation, and human activities, have had different regimes during the Holocene in climatically and topographically diverse regions of the world (Jenny et al., 2019; Zekollari et al., 2017). Multi-proxy (sedimentological, palynological, and geochemical) analyses have been widely employed in previous research to decode soil erosion processes response to past environmental changes (Bajard et al., 2017a; Barreiro-Lostres et al., 2017; Francke et al., 2019; Giguet-Covex et al., 2011). In recent years, human activity history has been reconstructed by sediment DNA, combined with other proxies, to reveal human impacts on soil erosion (Bajard et al., 2017b; Giguet-Covex et al., 2014). To better understand the roles of natural and anthropogenic factors on soil erosion processes, a long-term perspective is needed (Arnaud et al., 2016; Barreiro-Lostres et al., 2017).

Researchers have previously studied soil erosion processes at the 10,000 or 1000-year scale based on lake sediment records. Lake sediment is a crucial environmental archive, that provides valuable long-term continuous and high-resolution information. Undisturbed lake deposition records provide a natural experiment for study of complex interactions between topography, climate

change patterns, and land cover changes (Chen et al., 2014b; Sheng et al., 2015; Zhang et al., 2018a). Lake sediment, due to the processes that lead to its deposition, also gives insights about climate and anthropogenic forces over geological times affect

¹State Key Laboratory of Soil Erosion and Dryland Farming on Loess Plateau, Institute of Soil and Water Conservation, Northwest Agriculture and Forestry University; Chinese Academy of Sciences & Ministry of Water Resources, China

²Kunming Branch, Chinese Academy of Sciences, China

³State Key Laboratory of Estuarine and Coastal Research, East China Normal University, China

⁴Department of Geography, Faculty of Social Sciences, Hong Kong Baptist University, China

⁵Key Lab of Geographic Information Sciences of MOE, School of Geographic Sciences, Faculty of Geosciences, East China Normal University, China

Corresponding author:

Hongming He, State Key Laboratory of Soil Erosion and Dryland Farming on Loess Plateau, Institute of Soil and Water Conservation, Northwest Agriculture and Forestry University; Chinese Academy of Sciences and Ministry of Water Resources, 26 Xinong Road, Yangling, Shaanxi 712100, China.

Key Lab of Geographic Information Sciences of MOE, School of Geographic Sciences, Faculty of Geosciences, East China Normal University, 500 Dongchuan Road, Shanghai, 200241, China.
Emails: hongming.he@yahoo.com; hmhe@geo.ecnu.edu.cn

both soil erosion in the river basin and lake deposition (Bajard et al., 2015; Giguet-Covex et al., 2011). For sediment in closed and semi-enclosed lake basins, a portion of detached terrigenous material is transported and deposited in the lake. Previous research has used sediment physical, chemical, and biological indicators, through methods such as environmental magnetic susceptibility, particle size analysis, and elemental geochemical analysis, to reconstruct past environmental, and soil erosion processes (Arnaud et al., 2016; Bajard et al., 2015). Most of those studies were qualitative investigations, however, because it is not easy to calculate soil erosion rates. In this study, we combine simulation of soil erosion rates with analysis of lake deposition.

Yunnan province in southwestern China, combines a long history of human activity and environmental change with previous research on soil erosion and lake deposits, which provide the materials for this study. In the past three decades, the relationships between soil erosion and farming practices (Barton et al., 2004) and land use type and topography (Duan et al., 2015, 2020) in Yunnan have been analyzed by plot experiments and modeling. Spatial soil erosion distribution in this region has previously been analyzed based on observed data (Duan et al., 2020; Li et al., 2018). Much research also has been done on lake deposits in Yunnan Province, where there are a large number of tectonic fault lakes which were formed by tectonic movement in the Tibetan Plateau (Nanjing Institute of Geography and Limnology Chinese Academy of Sciences, 1989). Previous studies have shown that the main drivers of soil erosion changed greatly in Yunnan during the Holocene. The spatial distribution of soil erosion and factors that influence rates of erosion have also been investigated. However, the effect of long-term environmental changes on soil erosion are not clear.

Despite previous studies that provided sufficient materials for us to further investigate the processes of river basin soil erosion and lake deposition, there is little research that has attempted to study the variability of soil erosion processes affected by environment changes over the past in Yunnan, China. Therefore, the purpose of this study is analyze the responses of river basin soil erosion and lake deposition in Xingyun Lake, a shallow lake in Yunnan, during the Holocene. Those responses are calculated through quantitative approaches based on environmental proxies (i.e. precipitation, pollen, grain size, etc), land use cover, topography DEM, and other environmental factors. In this paper, sedimentary sequences are compared and analyzed, and the effects of erosional environmental changes on soil erosion and lake deposition are discussed.

Environmental setting

For this research, we selected Xingyun Lake in Yunnan Province to investigate the impacts of environmental changes on the processes of river basin soil erosion and lake deposition (Figure 1). Xingyun Lake is a shallow lake, with a surface area of 34.7 km² and a watershed area of 344.8 km². On its eastern side Xingyun Lake is connected with Fuxian Lake by the Ge River.

According to observations by the Yuxi meteorological station (20 km west of Xingyun Lake), average annual rainfall is 872 mm, and occurs mostly from May to October, accounting for more than 85% of the total annual rainfall. Area vegetation includes semi-humid evergreen broadleaf species, while the main species are *Pinus yunnanensis* and evergreen *Quercus* (Chen et al., 2014a). At present, large areas of paddy fields exist in the plain. The dominant soil type includes red soil, brown soil, purple soil, and paddy soils in Xingyun Lake (Li et al., 2018). The red soil is mainly distributed in the low mountain hills, accounting for 41.22% of the watershed area, while the purple soil is found least in the study area, mainly distributed in the Mesozoic strata outcrop area, accounting for 22.42% of the watershed area. In the past few decades, the Xingyun Lake area has become a rapidly expanding center of urbanization and industrialization, which has increased soil erosion.

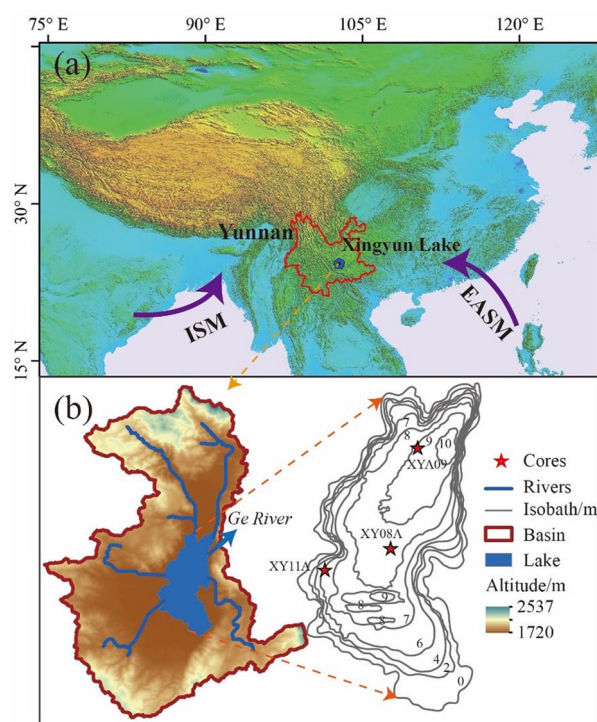


Figure 1. Location of the Xingyun Lake: (a) map showing the location of Xingyun Lake in the Asian summer monsoon system and (b) watershed topography and lake isobath from (Zhang et al., 2014), and locations of three cores.

Complex terrain and frequent extreme rainfall are the main natural factors generating strong soil erosion in Yunnan (Zhang et al., 2018b). Since Yunnan province is located on the southern margin of the Tibetan Plateau, there are serious regional soil erosion problems due to the complicated regional geological structure (Li et al., 2017). Soil erosion in Yunnan is a major environmental problem, which has caused declines in soil fertility (Barton et al., 2004). With more than 95% of the land surface containing mountains and valleys, and a large population, soil erosion will accelerate food insecurity because of farmland shortages (Duan et al., 2015).

To study soil erosion and lake deposition patterns during the Holocene, information about past climate and vegetation is needed. Fortunately, a variety of studies in Yunnan provide that needed information. In recent years, scholars have studied the Holocene environmental evolution of Yunnan lakes such as Tiancai Lake (Chen et al., 2014b; Xiao et al., 2014), Lugu Lake (Sheng et al., 2015; Zhang et al., 2018a), Erhai Lake (Shen et al., 2006), Qinghai Lake (Yang et al., 2016), and Xingyun Lake (Chen et al., 2014a; Hillman et al., 2017) (see locations in Figure 1b). Research using stalagmite (Dykoski et al., 2005) and sedimentary (Chen et al., 2020) records demonstrated obvious changes to the Indian Summer Monsoon (ISM) and East Asian Summer Monsoon (EASM) in the southwest, China (Figure 1a) during the Holocene, which affected vegetation history (Yang et al., 2016).

The past climate was characterized through time as cold and dry, warm and wet, and cold and dry. The climate changed from cold and dry to warm and wet at approximately 10.0 ka (1 ka = 1000 cal. a BP), and the monsoon activity increased after 10.0 ka, resulting in an increase of annual precipitation (Shen et al., 2006). The humid climate lasted until 4.6 ka in Tiancai Lake (Chen et al., 2014b) and Qinghai Lake (Yang et al., 2016), 5.5 ka in Xingyun Lake (Chen et al., 2014a), and 5.6 ka in Erhai Lake and Lugu Lake (Shen et al., 2006; Wang et al., 2017). Then the climate changed to drier gradually after the humid period.

Consequently, the vegetation in Yunnan changed along with climate changes. Pollen was used to reconstruct vegetation in

Table 1. AMS radiocarbon dates of sedimentary cores from Xingyun Lake.

Core name	Depth (cm)	Dating material	AMS ^{14}C age (^{14}C a BP)	Calibrated age (cal a BP)	Lab code	Data source
XY08A	47	Plant remains	265 ± 30	291 ± 133	XY-1A-24	(Chen et al., 2014a)
	228	Plant remains	1810 ± 30	1761 ± 52	XY-1A-(114-115)	
	300	Plant remains	3130 ± 30	3363 ± 28	XY-1B-(25-30)	
	377	Plant remains	5105 ± 25	5837 ± 75	XY-1B-66	
	411	Plant remains	5785 ± 25	6596 ± 43	XY-1B-83	
	437	Charcoal	6715 ± 35	7568 ± 46	XY-1B-96	
	477	Plant remains	7535 ± 30	8366 ± 20	XY-1B-116	
	485	Plant remains	7720 ± 40	8505 ± 85	XY-1B-120	
XY11A	5	Organic material	1335 ± 40	1310–1175	PA06849	(Zhang et al., 2014)
	167	Organic material	2485 ± 40	2725–2365	PA06850	
	209	Organic material	3625 ± 40	4080–3840	PA06851	
	221	Organic material	4645 ± 40	5570–5305	PA06852	
	243	Organic material	6210 ± 40	7250–7005	PA06853	
	303	Organic material	7375 ± 40	8325–8050	PA06854	
XYA09	37.5	Charcoal	110 ± 50	–4–277	71,482	(Hillman et al., 2017)
	145	Charcoal	1060 ± 25	928–1052	84,866	
	210.5	Leaf	1785 ± 35	1616–1817	141,232	
	263	Charcoal	2220 ± 20	2154–2328	84,815	
	310.5	Charcoal	3070 ± 15	3249–3357	122,325	
XYB08	408.5	Charcoal	4080 ± 20	4448–4796	141,234	
	446.5	Leaf	5665 ± 20	6364–6524	172,626	
	504.5	Leaf	7375 ± 35	8049–8343	141,235	

Table 2. The current datasets used to calculate the soil erosion.

Data type	Source	Description
Rainfall data	Annual rainfall data from 1986 to 2011 in Yuxi and Muli meteorological stations were obtained from China National Meteorological Data Sharing Platform (http://data.cma.cn).	Annual rainfall data was used to calculate rainfall erosivity factor (R) in RUSLE.
Soil	Soil erodibility factor was acquired from National Geographic Resource Science Sub Center (http://gre.geodata.cn), with a spatial resolution of 30 m.	Soil erodibility factor (K) is a one of factors in the soil erosion model.
Digital Elevation Model (DEM)	DEM data was derived from Google Earth, with a spatial resolution of 30 m.	DEM data was used to calculate the slope length and slope gradient factors (LS).
Landsat TM images	Landsat TM images were derived from Google Earth engine (https://earthengine.google.com/), with a spatial resolution of 30 m, from 1986 to 2011. We selected the least cloud (<10%) from July to September as the used image in this year.	We used Landsat TM images to calculate the vegetation cover and interpret land use type which for vegetation cover factor (C) and erosion control practice factor (P).

Tiancai Lake (Xiao et al., 2014), Qinghai Lake (Yang et al., 2016), Xingyun Lake (Chen et al., 2014a), and Erhai Lake (Shen et al., 2006). During the period of humid climate, the number of tropical plants, such as *Tsuga*, *Picea*, and *Pine* expanded, and the wood composition concentration increased, indicating an increase in vegetation coverage. The pollen concentration and wood proportion of decreased gradually from 5.5 to 4.6 ka in the above-mentioned four lakes, indicating that the vegetation coverage decreased (Yang et al., 2016).

Significant, intense human activity existed in Yunnan at least 6000 years ago according to sedimentological evidence (Hillman et al., 2018; Shen et al., 2006). According to historical literature, Yunnan's population increased significantly in three different times during the historical period (Dictionary, 1993; Li and Su, 1997). The first population peak was during the East Han Dynasty (i.e. 25–220 CE), when the population size reached 2.2 million and decreased at the end of this period. During the Nanzhao (738–902 CE) and Dali Kingdoms (937–1094 CE) (two local authorities in Yunnan), the population increased and remained at a stable level. After the Ming Dynasty (1368–1644 CE), the population increased sharply. As is known, an increased population needs more land to reclaim and supply food. The history of forest clearance recorded in Xingyun Lake has a long history exceeding 2000 years, and

increasing proportion of grass can be used as evidence for human impact due to forest clearance (Shen et al., 2006; Wu et al., 2014). From the information presented above, it is clear that environmental changes occurred in Yunnan during the Holocene.

Materials and methods

Data sources

In this study, modern soil erosion was calculated to calibrate and estimate soil erosion during the Holocene. Therefore, we collected multisource datasets, including paleoenvironment proxies and present-day datasets. Holocene lake sediment data were collected from published references and used to reconstruct sequences of paleoenvironment parameters (precipitation, vegetation, sediment rate, etc.) (Table 1). We used median calibrated radiocarbon ages calibrated using the INTCAL calibration curves from the original publications in our analysis. Three sediment cores were used to reconstruct paleotopography and calculate lake deposition rate in different periods.

Observed climate data, topography data, soil types, and remote sensing images (Landsat TM) were collected and processed for simulation of soil erosion in the river basin (Table 2). Annual

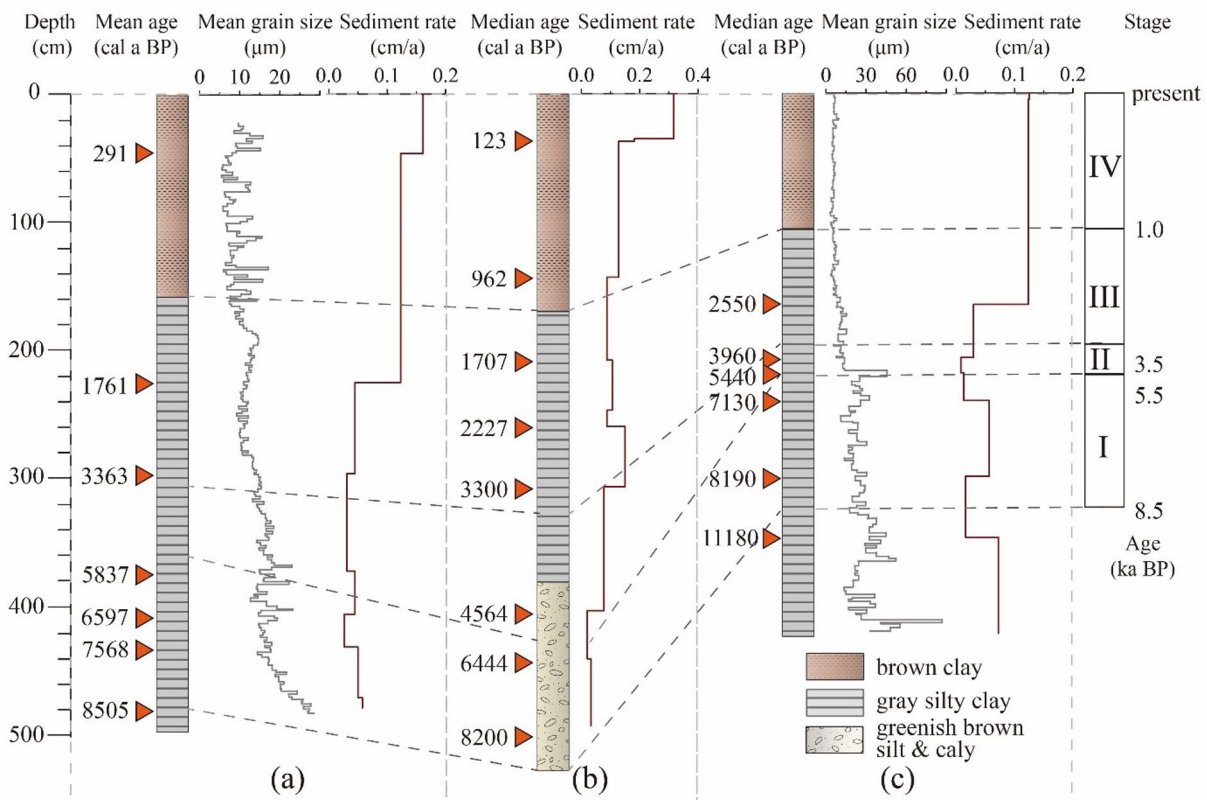


Figure 2. Sedimentary and stratigraphic features in Xingyun Lake: (a) XY08A (Chen et al., 2014a), (b) XYA09 (Hillman et al., 2014), and (c) XY11A (Zhang et al., 2014).

precipitation data from the Yuxi meteorological station, the nearest station to Xingyun Lake, were obtained from the China National Meteorological Data Sharing Platform (<http://data.cma.cn>). Digital Elevation Model (DEM) data with a spatial resolution of 30 m (downloaded from Google Earth Engine, <https://earthengine.google.com/>), was used to calculate the slope length and slope gradient factors for the soil erosion model. Landsat TM images with a spatial resolution of 30 m were selected from a period from July to September when cloud cover less than 10% each year from 1986 to 2011 (downloaded from Google Earth Engine, <https://earthengine.google.com/>). Land use data from the Landsat TM images were classified as water body, farmland, construction land, deciduous broadleaf forest (DEC), evergreen broadleaf forest (EVE), and coniferous forest (CON), using supervised methods and used to calculate the soil and water conservation measures factor in the soil erosion model. Soil erodibility, calculated from soil texture and amount of soil organic matter, was acquired from National Geographic Resource Science Sub-Center (<http://gre.geodata.cn>), with a spatial resolution of 30 m.

Soil erosion rates can be explained using the continuous Holocene record of sediment in Xingyun Lake. Based on mean grain size and sedimentation rate of the three sediment cores from Xingyun Lake (Figure 2), depositional processes in Xingyun Lake have been divided into four stages during the Holocene. The mean grain size was coarse from 8.5 to 5.5 ka (Stage 1), and it changed to fine particles with decreased deposition rate between 5.5 and 3.5 ka (Stage 2). Then, mean grain size changed to even finer with increased deposition rate from 3.5 to 1.0 ka (Stage 3), with dramatic fluctuations in mean grain size, with increased sediment rate since 1.0 ka to present (Stage 4).

Reconstruction of sequences of paleoenvironments proxies

In this study, the ratio of wood to pollen was used to represent vegetation cover during the Holocene according to estimates

from a pollen percentage diagram (Mehl and Hjelle, 2015; Sugita, 2007). Application of the REVEALS (Regional Estimates of Vegetation Abundance from Large Sites) model on pollen records to determine vegetation composition represents a significant advance in the quantification of past regional land cover (Sugita, 2007). The REVEALS model was developed to reconstruct quantitatively regional vegetation abundance from pollen assemblages and has been tested using actual vegetation in many lakes (Hellman et al., 2008; Sugita et al., 2010; Soepboer et al., 2016), which indicates that is a reliable model for reconstructing paleovegetation. The regional proportion of vegetation composition estimated from relative pollen yield is as follows:

$$\hat{V}_i = \frac{\frac{n_i}{\hat{a}_i K_i}}{\sum_{j=1}^m \left(\frac{n_j}{\hat{a}_j K_j} \right)} \quad (1)$$

where \hat{V}_i is vegetation proportion of tree species i , m is the number of tree species and n_i , \hat{a}_i and K_i are the pollen count, the estimate of relative pollen productivity, and the dispersal-deposition coefficient of the taxon i , respectively.

The main tree species in Xingyun Lake basin included *Tsuga*, *Pinus*, *Quercus*, and *Alnus* (Chen et al., 2014a), which constitute vegetation types of deciduous broadleaved forest, evergreen broadleaved forest, and coniferous forest. We used pollen assemblages to reconstruct the main tree species percentages corresponding to forest composition using equation (1). Precipitation for the Holocene, reconstructed from pollen data, came from previously published data (Chen et al., 2014a). Sediment particle size was verified to reflect hydrology conditions and soil erosion in certain lake watersheds (Wilhelm et al., 2015). In this study, we used the above sediment indexes to verify the validity of the soil erosion simulation.

Table 3. Annual environment parameters and soil erosion in ESEM.

Year	Precipitation (mm/a)	Vegetation cover	DEC	EVE	CON	Soil erosion by RUSLE (t/ha/a)	Soil erosion by ESEM (t/ha/a)
1988	848.60	0.71	0.25	0.42	0.33	219.59	220.22
1989	798.30	0.73	0.16	0.53	0.31	236.90	253.43
1991	1001.00	0.76	0.45	0.29	0.26	284.54	332.32
1992	702.50	0.66	0.16	0.54	0.30	131.14	128.94
1993	875.10	0.73	0.26	0.31	0.42	251.70	254.30
1994	871.40	0.67	0.48	0.17	0.35	178.19	166.41
1995	957.60	0.71	0.16	0.47	0.37	254.98	255.21
1996	882.10	0.65	0.31	0.36	0.34	137.51	138.90
1997	1083.60	0.70	0.19	0.49	0.32	231.94	260.90
1998	876.00	0.71	0.12	0.64	0.24	208.07	246.24
1999	1125.00	0.68	0.16	0.50	0.35	290.55	231.80
2000	894.40	0.69	0.17	0.57	0.26	189.49	201.78
2001	1084.80	0.72	0.16	0.51	0.33	271.41	297.97
2003	957.10	0.70	0.22	0.49	0.29	209.88	237.23
2004	884.90	0.68	0.22	0.53	0.26	168.64	194.72
2005	814.30	0.71	0.38	0.29	0.33	185.72	222.12
2006	804.10	0.67	0.31	0.12	0.57	115.01	138.44
2007	881.30	0.69	0.27	0.25	0.48	164.05	180.60
2008	967.90	0.70	0.29	0.24	0.48	169.61	207.97
2009	628.40	0.68	0.16	0.57	0.27	114.92	141.69
2010	639.60	0.65	0.37	0.28	0.35	93.17	112.15
2011	599.60	0.67	0.37	0.27	0.37	110.56	142.63

Quantification of soil erosion and lake deposition

In the lake system, soil erosion occurred when terrestrial detritus was removed from land, transported, and eventually deposited in the lake. Previous research has described a few methods for quantifying relationships between erosion in drainage areas with sediment accumulation in lakes (Bajard et al., 2017a; Barreiro-Lostres et al., 2017). It is difficult to quantify relationships between soil erosion and deposition in a drainage basin because methods for estimating erosion rate are often based on deposition rates. In this research, however, we calculated the erosion rate and deposition rate using two different methods.

Calculation of soil erosion intensity. Soil erosion is a complex earth surface process affected by natural and anthropogenic factors, such as precipitation, vegetation, soil, topography, and human activity. Spatial and temporal environmental data can be used to simulate soil erosion on a watershed scale (Chandramohan et al., 2015). However, it is challenging to reconstruct some spatial and temporal environmental parameters, such as vegetation cover and precipitation.

We calculated soil erosion during the Holocene based on the relationship between the modern soil erosion rate and environmental parameters. First, we used the Revised Universal Soil Loss Equation (RUSLE), which has been widely used to calculate soil erosion around the world (Hussein et al., 2016; Renard et al., 1997), to calculate the erosion rate in the Xinyun Lake basin from 1986 to 2011. The structure of RUSLE is as follows:

$$E = R \cdot K \cdot L \cdot S \cdot C \cdot P \quad (2)$$

where E is the estimated annual soil loss ($\text{t ha}^{-1} \text{a}^{-1}$). R is the rainfall erosivity factor, and represents the potential erosive capability of a rain event ($\text{MJ mm ha}^{-1} \text{a}^{-1}$), based on the intensity and duration of rainfall in a given geographical area. K is the soil erodibility factor ($\text{t ha h}^{-1} \text{MJ}^{-1} \text{mm}^{-1}$). L is the slope length and S is the gradient factor, two dimensionless topography factors determined by the length and steepness of a slope. C is the vegetation cover factor and P is the erosion control practice factor. The K , L , S , C , and P factors in this study were calculated using previously validated methods (Li et al., 2018).

Once we have modern soil erosion rates, then we turn toward modeling soil erosion rates in the Holocene. We propose some preliminary assumptions to satisfy the model simulation while recognizing the RUSLE application's parameters and boundary limitations to environmental changes. Since we assume that the soil erodibility (K) and topography factors (L and S) have not changed significantly and we acknowledge that the conservation practice factor (P), is difficult to calculate in the past, those factors are omitted from the model. Thus, rainfall and vegetation are recognized as the main variables that affect soil erosion and we decided to use annual precipitation, vegetation cover, and forest composition (deciduous broadleaved trees, evergreen broadleaved trees, and coniferous trees). A statistical regression model was calculated to reconstruct the relationship between soil erosion and environmental parameters based on modern annual data (1986–2011) (Table 3). The estimated soil erosion model (ESEM) works as follows:

$$E_c = 0.36Pre * EVE + 1566.26Ver + 493.08DEC^2 + 263.73CON - 1136.66 \quad (3)$$

where E_c is the calculated average annual soil erosion rate ($\text{t ha}^{-1} \text{a}^{-1}$), Pre is annual precipitation (mm), Ver is vegetation coverage, DEC , EVE , and CON are the proportion of deciduous broadleaved trees, evergreen broadleaved trees, and coniferous trees in forests, respectively. We calculated soil erosion during the Holocene with the ESEM and reconstructed environmental parameter sequences.

Calculation of lake deposition rate. A detailed sediment depositional process is key for calculating lake sediment deposition recognized as sediment fluxes. For that calculation, we need to identify the topography of the lakebed for each sediment interval analyzed in the sediment cores. We used the detailed present-day isobath and three sediment chronology (Figures 1b and 2) to reconstruct the lake topography during the main periods (Figure 3), using the tool of TIN (Triangulated Irregular Network) in ArcGIS, assuming that water level remained unchanged in the Holocene. Sedimentation volume was calculated using ArcGIS for each sediment interval based on lake topography and total sediment volume. Average deposition rate was calculated from accumulated mass, dry bulk density, and integrated according to time (T):

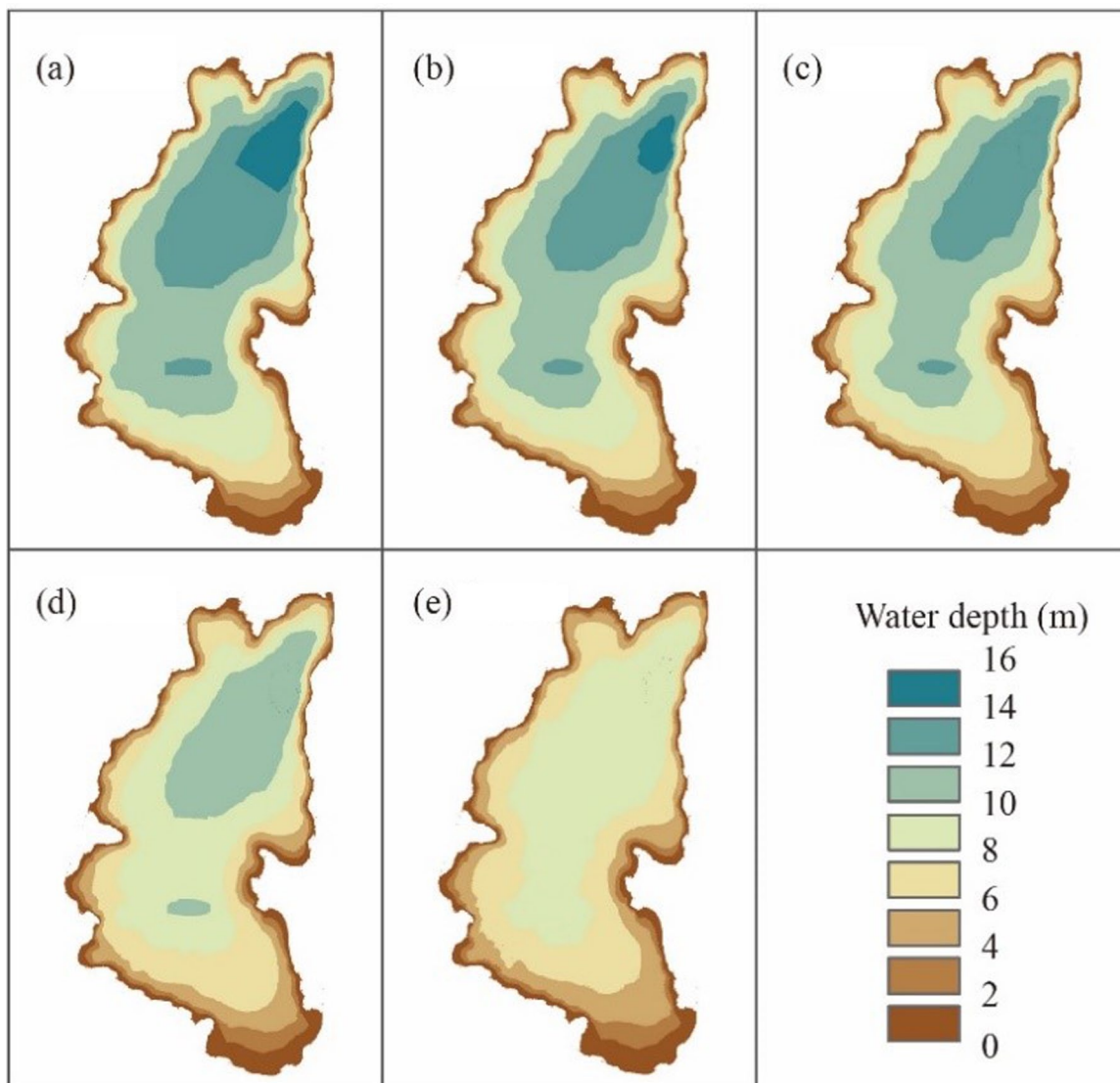


Figure 3. Sediment deposition process in Xinyun Lake: (a) 8.5 ka, (b) 5.5 ka, (c) 3.5 ka, (d) 1.0 ka, and (e) present.

$$S_r = \frac{Mv * \rho_s}{T} \quad (4)$$

where S_r is the lake deposition modulus ($t a^{-1}$); Mv is accumulated mass during the interval time (m^3); ρ_s is the dry soil bulk density ($t m^{-3}$), converted from the published data in literature (Hillman et al., 2017); T is interval time (a).

Correlation of soil erosion and lake deposition. To further verify the mechanism of erosion-deposition and factors, we carried out statistical analysis using the Pearson correlation coefficient (SPSS 23.0).

Results

Soil erosion and lake deposition sequences were reconstructed based on multiple proxies in Holocene in Xingyun Lake (Figure 4). According to the estimated precipitation (Figure 4a), the climate surrounding Xingyun Lake can be divided into stages. The climate became wetter from 8.5 ka, while the wettest period in Xingyun Lake was recorded right before 5.5 ka, when annual precipitation reached 1400 mm, much higher than the present. The climate became gradually drier after 5.5 ka, and unstable after 2.0 ka.

Vegetation cover changed synchronously with precipitation in the Xingyun Lake catchment (Figure 4b). The highest amount of

vegetation cover occurred between 8.5 and 5.5 ka, with an average cover rate of more than 70%. After 5.5 ka, vegetation cover decreased gradually until 2.2 ka. Vegetation cover fluctuated, which was similar to the fluctuations of precipitation after 2.2 ka, and a peak high vegetation cover occurred around 1.2 ka.

Forest composition changed since 8.5 ka in the Xingyun Lake catchment (Figure 4c). Generally, the changes in the evergreen broadleaved forest were similar to changes in the coniferous forest. The proportion of deciduous broadleaved forest was far less than the other types, and did not exceed 15% during this period. However, three peaks of deciduous broadleaved forest occurred in 5.6, 3.6, and 0.8 ka.

The Holocene soil erosion rate was calculated using the ESEM model. The soil erosion rate has decreased since 8.5 ka (Figure 4d). The most intensive soil erosion occurred from 7.4 to 7.0 ka, when the soil erosion rate reached $378.15 t ha^{-1} a^{-1}$. After 6.2 ka, the soil erosion rate decreased gradually, and this tendency continued until 2.6 ka. Unstable changes also occurred after 2.6 ka, and the soil erosion rate increased from 2.6 to 1.0 ka, then decreased after 1.0 ka.

The lake deposition process was calculated using the sedimentation rate and lake topography in Xingyun Lake. The stable deposition rate (Figure 4f) occurred during Stage I, when the average rate was $3.18 \times 10^6 t a^{-1}$. During Stage II, the deposition rate slowed, and the lowest rate occurred from 5.2 to 4.8 ka. After

3.5 ka, the deposition rate generally increased. However, a decrease in deposition occurred from 1.4 to 1.2 ka. In Stage IV, the deposition rate increased significantly and the highest value (27.96 t a^{-1}) was reached in 0.2 ka.

To further verify the mechanism of erosion-deposition and factors, we carried out statistical analysis using the Pearson correlation coefficient. The results are displayed in Table 4.

Discussion

In this study, we reconstructed soil erosion and lake deposition sequences during the Holocene of Xingyun in Yunnan, China based on current observed data and paleoenvironment proxies. It is important to analyze trends found in both river basin soil erosion and lake sediment deposition from the perspective of climate change and human activities.

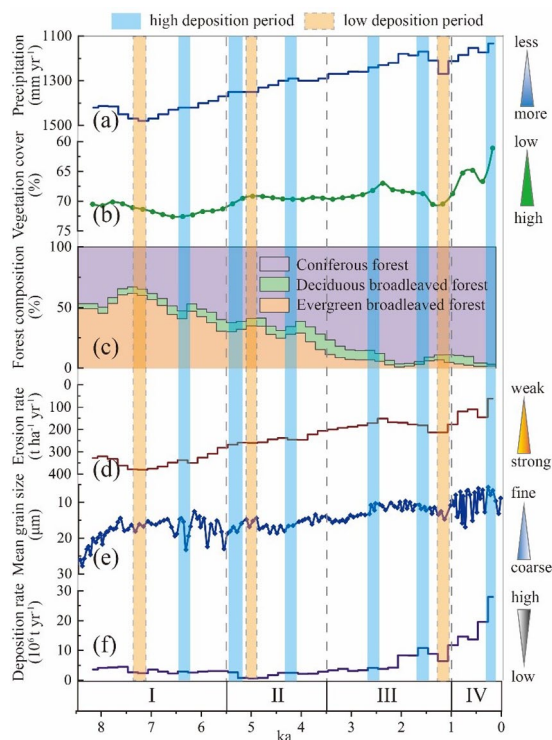


Figure 4. Reconstruction of past soil erosion and lake deposition: (a) annual precipitation reconstruction based on pollen (Chen et al., 2014a). (b) vegetation cover, (c) forest composition reconstructed from pollen of core XY08A, (d) erosion rate, (e) mean grain size of core XY08A, and (f) deposition rate.

Driving factor of erosion and deposition

From the previous analysis, the history of climate change during the Holocene in the Xingyun Lake basin can be divided into four stages (Figure 2). During Stage I, ISM and EASM activity increased, increasing annual precipitation (Chen et al., 2014b; Shen et al., 2006). During Stage II, the climate was warm and humid. According to estimated precipitation sequences, the average annual precipitation for Xingyun Lake during this stage was 1474 mm, corresponding to the highest precipitation amounts on record in Yunnan (Chen et al., 2014a; Yang et al., 2016). After Stage II, the climate became drier and fluctuated. Changing vegetation patterns in the Xingyun Lake basin (Figure 4b and c) were synchronous and corresponded with the estimated precipitation. We conclude that the Holocene vegetation in the lake basin was mainly affected by climate change, and the vegetation experienced the same pattern of changes as the climate.

The processes of soil erosion, sediment transport, and deposition was integral in the lake system. According to our results, soil erosion was mainly affected by precipitation and vegetation conditions. However, there was an opposite relationship between the deposition rate and erosion rate in the Xingyun Lake basin during the Holocene. Rainfall-runoff conditions were the main factors influencing soil erosion, sediment transport, and deposition. Sediment particle size in core XY08A, which was drilled in the center of Xingyun Lake (Chen et al., 2014a) can be recognized as a proxy indicator of hydrology condition. According to Figure 4, the Holocene sedimentary mean grain size (Figure 4e) was consistent with the estimated precipitation (Figure 4a), vegetation (Figure 4b), and erosion (Figure 4d). Therefore, we could surmise that runoff was affected by the amount of precipitation. Partially coarse soil particles were deposited in the lake during the high precipitation period in the Holocene.

However, the sequences of deposition rates are opposite to the erosion rate and rainfall-runoff conditions in the Xingyun Lake basin. Vegetation coverage is an essential factor affecting soil erosion and sediment transport (Huang et al., 2016). According to Figure 4, the changing deposition rate corresponded to changes in vegetation cover and wood proportion of pollen. High deposition rates occurred during the periods of sparse forest vegetation and dominant grassland. The soil erosion rate for grassland is far greater than that for forested land in Yunnan (Duan et al., 2020; Li et al., 2018). Generally, topsoil is easily eroded by rainfall-runoff in grassland areas (Evans et al., 2017). According to previous research, significantly small soil particles eroded during short periods of rainfall in grassland areas due to sheet flow erosion (Hao et al., 2019). This shows that the mean grain sizes were correlated to vegetation trends and corresponded with deposition in Xingyun Lake.

Table 4. Person correlation coefficient of erosion and deposition factors in Xingyun Lake.

	Precipitation	Herb	EVE	DEC	CON	Grain size	Erosion	Deposition
Precipitation								
Herb	-0.80**							
EVE	0.97**	-0.67**						
DEC	0.15	-0.21	0.03					
CON	-0.97**	0.71**	-0.99**	-0.16				
Grain size	0.82**	-0.73**	0.77**	0.29	-0.79**			
Erosion	0.97**	-0.86**	0.96**	0.04	-0.95**	0.79**		
Deposition	-0.65**	0.77**	-0.53**	-0.49**	0.59**	-0.70**	-0.63**	

**Significantly correlated at the 0.01 level (bilateral) level. Herb is the proportion of pollen. EVE, DEC, and CON are the proportion of evergreen broadleaved forest, deciduous broadleaved forest, and coniferous forest in woody respectively.

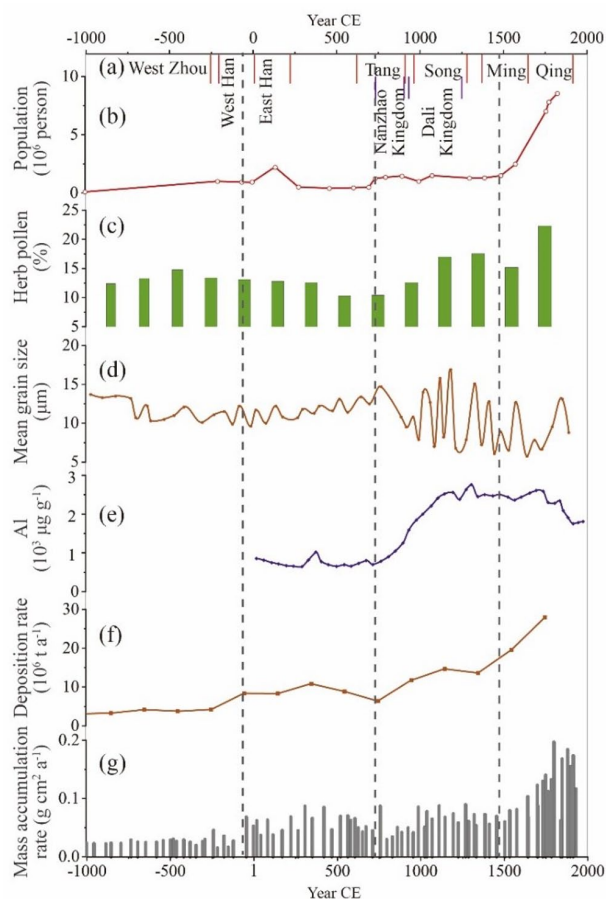


Figure 5. Records of human activity and lake deposition in Xingyun Lake: (a) Chinese Dynasty and two local authorities of Nanzhao and Dali Kingdom in the Yunnan, (b) population history in Yunnan (after (Dictionary, 1993; Li and Su, 1997)), (c) herbs proportion of pollen from core XY08A (Chen et al., 2014a), (d) mean grain size of core XY08A, (e) concentration of aluminum from core XYA09 (Hillman et al., 2014), (f) deposition rate, and (g) mass accumulation rate from core XYA09 (Hillman et al., 2017). Common Era (CE) ages of (c) and (d) were calculated from the calibrated (cal.) AMS ^{14}C ages based on 1950 CE.

The Pearson correlation coefficient for the relationship between soil erosion and lake deposition in Xingyun Lake (Table 4) shows a strong correlation between erosion, deposition, precipitation, and vegetation. The proportion of herb pollen, mean grain size, and erosion rate were well correlated with the deposition rate, revealing those factors are related to the erosion-deposition processes. Therefore, we determined that more fine particle materials were eroded during the periods of dry climate and grass development, resulting in a high amounts of deposition during those dry periods.

The processes of soil erosion, sediment transportation and lake deposition are complex, resulting in complexity and uncertainty in the research (Pandey et al., 2016). A few proxies of lake sediment were used to capture the erosion signal in other studies, however, it is difficult to understand the complex relationships between climate, vegetation, human, and the earth system in general (Arnaud et al., 2016; Bajard et al., 2017b; Giguet-Covex et al., 2011). In this study, we attempted to reconstruct the process of soil erosion using the estimated soil erosion model (ESEM). The results show good consistency with sediment grain size and lake deposition rate (Figure 4). Combined with the relativity principles of soil erosion, we determined that the simulated results are reliable. However, the simulated results are based on reconstructed paleoenvironment parameters (precipitation, vegetation cover and composition), which are not widely recognized. For

example, precipitation was estimated to be 69% higher from 8.6 to 6.0 ka (1474 mm) than the present-day average (872 mm) in the Xingyun Lake basin (Chen et al., 2014a), although those estimations are disputed by other scholars (Hillman et al., 2018). The reliability of the reconstructed environment sequences creates uncertainty in the simulation results. In addition, the interaction of processes of soil erosion and lake deposition need to be further investigated through an integrated model acquired from more extensive case studies.

Lake erosion and human activity

Soil erosion has been exacerbated by human activity, such as deforestation and land reclamation. We used the herb proportion of pollen to evaluate the degree of forest clearance by human activity. The herb proportion of pollen increased in 760 and 1600 CE in Xingyun Lake (Figure 5c), the last two times the population increased. Decreasing soil aggregate stability and particle size resulted from conversion of natural forest to cropland (Beheshti et al., 2012; Duan et al., 2021; Li et al., 2021), which caused the decreased particle size of the topsoil to be easily eroded. The mean grain size of lake sediment decreased in 760 and 1600 CE (Figure 5d), corresponding with periods of population growth and land reclamation. In addition, there is a long history of mineral resource extraction in the Xingyun watershed (Hillman et al., 2014). Concentration of aluminum (Al) in the lake sediment sharply increased after the Nanzhao and Dali Kingdoms periods (Figure 5e), indicating intensive activities of resource extraction.

Soil erosion and lake deposition are affected by human activity. The lake deposition rate (Figure 5f) and mass accumulation (Figure 5g) increased in Xingyun Lake during the last 3000 years. Three periods of quick increases occurred during the East Han Dynasty, Nanzhao Kingdoms, and Ming Dynasty, which corresponds with population expansion. Therefore, we conclude that human activity in the Xingyun Lake basin had apparent impacts on soil erosion and lake deposition through land reclamation and resource extraction since the East Han Dynasty, which was exacerbated during the Nanzhao Kingdoms and Ming Dynasty.

Compared with other lakes around the world, apparent impacts on lake basin soil erosion from human activity appears between 200 BCE and 400 CE in the northern French Alps (Arnaud et al., 2016), 700 CE in central Mexico (Castillo et al., 2017), and about 1000 CE in central Spain (Barreiro-Lostres et al., 2017). The history of lake basin soil erosion differs by environment and human activities around the world (Bajard et al., 2017a). Lugu Lake, also located in Yunnan, but at a relatively high elevation, has a shorter history of apparent human impacts on lake environment of less than 700 years (Wang et al., 2020). However, there is no effective method to study the degree of human impact on lake basin soil erosion and deposition. Nine other large lakes in Yunnan, with different elevations, climates, and vegetation and human settlement histories, would provide a possibility to study the human impacts on lake history further.

Conclusion

Based on the Holocene sedimentary records of Xingyun Lake in Yunnan, China, we reconstructed the sequences of main drivers of soil erosion and further investigated interactions between climate change, human activity, soil erosion, and lake deposition during the Holocene. More fine particle materials eroded during periods when the climate was dry and herbaceous plants developed, resulting in high amounts of deposition in the lake. The lake deposition rate increased during the East Han Dynasty, Nanzhao Kingdoms, and Ming Dynasty caused by population expansion through land reclamation and resource extraction in the lake basin. This

study provides new insights to investigate soil erosion and lake deposition effected by anthropogenic impacts and climate forcing on a millennium timescale. It is noteworthy that the reliability of the reconstructed environment sequences creates uncertainty in the simulation results. In our future work, more lakes and high-resolution data will be investigated to better understand the relationships between humans and climate in terms of river basin erosion and lake deposition processes.

Author contributions

Hongfei Zhao and Hongming He collected the research data, analyzed data and wrote original draft preparation. Jie Zhou, Qianli Sun, Claudio O. Delang and Hongming He designed the research and provided suggestion for improving the manuscript. Ali Mokhtar and Yue Ma generated the figures in the main text. Claudio O. Delang polished the language. All authors modified the final manuscript.

Availability of data and materials

All data in this study can be provided upon request.

Declaration of conflicting interests

The author(s) declared no potential conflicts of interest with respect to the research, authorship, and/or publication of this article.

Funding

The author(s) disclosed receipt of the following financial support for the research, authorship, and/or publication of this article: This work was partially supported by the Second Tibetan Plateau Scientific Expedition and Research Program (Grant No. SQ2019QZ-KK2003), National Key R&D Program of China [grant number: 2017YFC0505200] and the National Natural Science Foundation of China [grant number: 41672180], the Strategic Priority Research Program of the Chinese Academy of Sciences (Grant No. XDA23020603), the Science & Technology Basic Resources Investigation Program of China (Grant No. 2017FY101303), the Key Platforms and Scientific Research Projects in Universities in Guangdong Province of China (Grant No. 2018KTSCX212) and the Guangdong Rural Science and Technology Commissioner Project of China (Grant No. 319B0203).

ORCID iD

Hongfei Zhao  <https://orcid.org/0000-0001-9507-3162>

References

- Arnaud F, Poulencard J, Giguët-Covex C et al. (2016) Erosion under climate and human pressures: An alpine lake sediment perspective. *Quaternary Science Reviews* 152: 1–18.
- Bajard M, Poulencard J, Sabatier P et al. (2017a) Progressive and regressive soil evolution phases in the Anthropocene. *Catena* 150: 39–52.
- Bajard M, Poulencard J, Sabatier P et al. (2017b) Long-term changes in alpine pedogenetic processes: Effect of millennial agro-pastoralism activities (French-Italian Alps). *Geoderma* 306: 217–236.
- Bajard M, Sabatier P, David F et al. (2015) Erosion record in Lake La Thuile sediments (Prealps, France): Evidence of montane landscape dynamics throughout the Holocene. *The Holocene* 26: 350–364.
- Barreiro-Lostres F, Moreno A, González-Sampériz P et al. (2017) Erosion in Mediterranean mountain landscapes during the last millennium: A quantitative approach based on lake sediment sequences (Iberian Range, Spain). *Catena* 149: 782–798.
- Barton AP, Fullen MA, Mitchell DJ et al. (2004) Effects of soil conservation measures on erosion rates and crop productivity on subtropical Ultisols in Yunnan Province, China. *Agriculture, Ecosystems & Environment* 104: 343–357.
- Beheshti A, Raiesi F and Golchin A (2012) Soil properties, C fractions and their dynamics in land use conversion from native forests to croplands in northern Iran. *Agriculture, Ecosystems & Environment* 148: 121–133.
- Castillo M, Muñoz-Salinas E, Arce JL et al. (2017) Early Holocene to present landscape dynamics of the tectonic lakes of west-central Mexico. *Journal of South American Earth Sciences* 80: 120–130.
- Chandramohan T, Venkatesh B and Balchand AN (2015) Evaluation of three soil erosion models for small watersheds. *Aquatic Procedia* 4: 1227–1234.
- Chen FH, Chen XM, Chen JH et al. (2014a) Holocene vegetation history, precipitation changes and Indian Summer Monsoon evolution documented from sediments of Xingyun Lake, south-west China. *Journal of Quaternary Science* 29: 661–674.
- Chen X, Li YL, Metcalfe S et al. (2014b) Diatom response to Asian monsoon variability during the Late Glacial to Holocene in a small treeline lake, SW China. *The Holocene* 24: 1369–1377.
- Chen XM, Wu D, Huang XZ et al. (2020) Vegetation response in subtropical southwest China to rapid climate change during the Younger Dryas. *Earth-Science Reviews* 201: 103080.
- Dictionary EBOY (1993) *Yunnan Dictionary*. Kunming, China: Yunnan People's Publishing House. (in Chinese).
- Dotterweich M (2013) The history of human-induced soil erosion: Geomorphic legacies, early descriptions and research, and the development of soil conservation—A global synopsis. *Geomorphology* 201: 1–34.
- Duan LX, Sheng H, Yuan H et al. (2021) Land use conversion and lithology impacts soil aggregate stability in subtropical China. *Geoderma* 389: 114953.
- Duan XW, Bai ZW, Rong L et al. (2020) Investigation method for regional soil erosion based on the Chinese Soil Loss Equation and high-resolution spatial data: Case study on the mountainous Yunnan Province, China. *Catena* 184: 104237.
- Duan XW, Rong L, Zhang GL et al. (2015) Soil productivity in the Yunnan province: Spatial distribution and sustainable utilization. *Soil and Tillage Research* 147: 10–19.
- Dykoski CA, Edwards RL, Cheng H et al. (2005) A high-resolution, absolute-dated Holocene and deglacial Asian monsoon record from Dongge Cave, China. *Earth and Planetary Science Letters* 233: 71–86.
- Evans R, Collins AL, Zhang Y et al. (2017) A comparison of conventional and ¹³⁷Cs-based estimates of soil erosion rates on arable and grassland across lowland England and Wales. *Earth-Science Reviews* 173: 49–64.
- Francke A, Dosseto A, Panagiotopoulos K et al. (2019) Sediment residence time reveals Holocene shift from climatic to vegetation control on catchment erosion in the Balkans. *Global and Planetary Change* 177: 186–200.
- Giguët-Covex C, Arnaud F, Poulencard J et al. (2011) Changes in erosion patterns during the Holocene in a currently treeless subalpine catchment inferred from lake sediment geochemistry (Lake Anterne, 2063 m a.s.l., NW French Alps): The role of climate and human activities. *The Holocene* 21: 651–665.
- Giguët-Covex C, Pansu J, Arnaud F et al. (2014) Long livestock farming history and human landscape shaping revealed by lake sediment DNA. *Nature Communications* 5: 3211.
- Hao HX, Wang JG, Guo ZL et al. (2019) Water erosion processes and dynamic changes of sediment size distribution under the combined effects of rainfall and overland flow. *Catena* 173: 494–504.
- Hellman S, Gaillard M-J, Broström A et al. (2008) The REVEALS model, a new tool to estimate past regional plant abundance from pollen data in large lakes: Validation in southern Sweden. *Journal of Quaternary Science* 23: 21–42.

- Hillman AL, Abbott MB, Finkenbinder MS et al. (2017) An 8,600 year lacustrine record of summer monsoon variability from Yunnan, China. *Quaternary Science Reviews* 174: 120–132.
- Hillman AL, Abbott MB and Yu JQ (2018) Climate and anthropogenic controls on the carbon cycle of Xingyun Lake, China. *Palaeogeography, Palaeoclimatology, Palaeoecology* 501: 70–81.
- Hillman AL, Yu JQ, Abbott MB et al. (2014) Rapid environmental change during dynastic transitions in Yunnan Province, China. *Quaternary Science Reviews* 98: 24–32.
- Huang W, Ho HC, Peng YY et al. (2016) Qualitative risk assessment of soil erosion for karst landforms in Chahe town, Southwest China: A hazard index approach. *Catena* 144: 184–193.
- Hussein MH, Amien IM and Kariem TH (2016) Designing terraces for the rainfed farming region in Iraq using the RUSLE and hydraulic principles. *International Soil and Water Conservation Research* 4: 39–44.
- Jenny JP, Koirala S, Gregory-Eaves I et al. (2019) Human and climate global-scale imprint on sediment transfer during the Holocene. *Proceedings of the National Academy of Sciences of the United States of America* 116: 22972.
- Li HQ, Yao YF, Zhang XJ et al. (2021) Changes in soil physical and hydraulic properties following the conversion of forest to cropland in the black soil region of Northeast China. *Catena* 198: 104986.
- Li S and Su PM (1997) A review of historical population in Yunnan. *Journal of Yunnan Normal University* 29: 23–29 (in Chinese).
- Li YJ, Liu SF, Chen LW et al. (2017) Mechanism of crustal deformation in the Sichuan-Yunnan region, southeastern Tibetan Plateau: Insights from numerical modeling. *Journal of Asian Earth Sciences* 146: 142–151.
- Li YM, Duan YP, Zhu J et al. (2018) The spatial distribution of soil erosion in the Xingyun lake basin based on GIS and RUSLE. *Science Technology and Engineering* 18: 34–42 (in Chinese with English abstract).
- Mehl IK and Hjelle KL (2015) From pollen percentage to regional vegetation cover — A new insight into cultural landscape development in western Norway. *Review of Palaeobotany and Palynology* 217: 45–60.
- Nanjing Institute of Geography and Limnology Chinese Academy of Sciences (1989) *Lake Environment and Deposition of Yunnan Province*. Beijing, China: Science Press. (in Chinese).
- Nearing MA, Xie Y, Liu BY et al. (2017) Natural and anthropogenic rates of soil erosion. *International Soil and Water Conservation Research* 5: 77–84.
- Pandey A, Himanshu SK, Mishra SK et al. (2016) Physically based soil erosion and sediment yield models revisited. *Catena* 147: 595–620.
- Renard KG, Foster GR, Weesies GA et al. (1997) Predicting soil erosion by water: A guide to conservation planning with the revised universal soil loss equation (RUSLE). Washington, DC: USDA Agriculture Handbook.
- Shen J, Jones RT, Yang XD et al. (2006) The Holocene vegetation history of Lake Erhai, Yunnan province southwestern China: The role of climate and human forcings. *The Holocene* 16: 265–276.
- Sheng EG, Yu KK, Xu H et al. (2015) Late-Holocene Indian summer monsoon precipitation history at Lake Lugu, northwestern Yunnan Province, southwestern China. *Palaeogeography, Palaeoclimatology, Palaeoecology* 438: 24–33.
- Soepboer W, Sugita S, Lotter AF et al. (2016) Pollen productivity estimates for quantitative reconstruction of vegetation cover on the Swiss Plateau. *The Holocene* 17: 65–77.
- Sugita S (2007) Theory of quantitative reconstruction of vegetation I: Pollen from large sites REVEALS regional vegetation composition. *The Holocene* 17: 229–241.
- Sugita S, Parshall T, Calcote R et al. (2010) Testing the Landscape Reconstruction Algorithm for spatially explicit reconstruction of vegetation in northern Michigan and Wisconsin. *Quaternary Research* 74: 289–300.
- Wang Q, Anderson NJ, Yang XD et al. (2020) Interactions between climate change and early agriculture in SW China and their effect on lake ecosystem functioning at centennial timescales over the last 2000 years. *Quaternary Science Reviews* 233: 106238.
- Wang Q, Yang XD, Anderson NJ et al. (2017) Direct versus indirect climate controls on Holocene diatom assemblages in a sub-tropical deep, alpine lake (Lugu Hu, Yunnan, SW China). *Quaternary Research* 86: 1–12.
- Wilhelm B, Sabatier P and Arnaud F (2015) Is a regional flood signal reproducible from lake sediments? *Sedimentology* 62: 1103–1117.
- Wu D, Zhou AF, Liu JB et al. (2014) Changing intensity of human activity over the last 2,000 years recorded by the magnetic characteristics of sediments from Xingyun Lake, Yunnan, China. *Journal of Paleolimnology* 53: 47–60.
- Xiao XY, Haberle SG, Shen J et al. (2014) Latest Pleistocene and Holocene vegetation and climate history inferred from an alpine lacustrine record, northwestern Yunnan Province, southwestern China. *Quaternary Science Reviews* 86: 35–48.
- Yang YP, Zhang HC, Chang FQ et al. (2016) Vegetation and climate history inferred from a Qinghai Crater Lake pollen record from Tengchong, southwestern China. *Palaeogeography, Palaeoclimatology, Palaeoecology* 461: 1–11.
- Zekollari H, Lecavalier BS and Huybrechts P (2017) Holocene evolution of Hans Tausen Iskappe (Greenland) and implications for the palaeoclimatic evolution of the high Arctic. *Quaternary Science Reviews* 168: 182–193.
- Zhang WX, Ming QZ, Shi ZT et al. (2014) Lake sediment records on climate change and human activities in the Xingyun Lake catchment, SW China. *PLoS One* 9: e102167.
- Zhang WX, Niu J, Ming QZ et al. (2018a) Holocene climatic fluctuations and periodic changes in the Asian southwest monsoon region. *Journal of Asian Earth Sciences* 156: 90–95.
- Zhang XQ, Hu MC, Guo XY et al. (2018b) Effects of topographic factors on runoff and soil loss in Southwest China. *Catena* 160: 394–402.